AIAA JOURNAL
Vol. 33, No. 1, January 1995

Effects of Streamwise Vorticity Injection on a Plane Turbulent Wake

James H. Weygandt*
Stanford University, Stanford, California 94305
and
Rabindra D. Mehta†
Stanford University/NASA Ames Research Center, Moffett Field, California 94035

Past flow visualization investigations of plane wakes originating from laminar initial boundary layers have shown the presence of streamwise vortical structures riding among the spanwise (von Kármán) vortices. Quantitative measurements of the mean streamwise vorticity were recently obtained which shed more light on their formation and subsequent evolution. Measurements made in the same wake with both initial boundary layers turbulent, however, showed that spatially stationary streamwise structures did not exist in this case, thus resulting in a distinctly different mean three-dimensional structure and streamwise evolution. In the present study, the effects of injecting streamwise vorticity on the structure and development of a wake originating from turbulent boundary layers are investigated. A corrugated extension attached to the splitter plate trailing edge produced a relatively strong array of counter-rotating pairs of streamwise vorticity which were injected into the turbulent wake. This resulted in large spanwise variations in the wake mean properties and Reynolds stress distributions. Although the mean streamwise vorticity decreased with downstream distance, the spanwise variations were found to persist into the far-field region ($X/\Theta > 500$) of the wake. In the near-field region ($X/\Theta < 500$), the wake growth was increased, and the velocity defect was reduced, both because of increased entrainment due to the injected vorticity. However, in the far-field region, the forced wake growth rate and peak Reynolds stresses were reduced significantly with respect to the undisturbed wake. This result is attributed to the effect of the relatively strong streamwise vorticity in making the spanwise structures more three dimensional and, hence, less efficient at entraining surrounding fluid.

Nomenclature

b	= wake half-width
C_f	= boundary-layer skin friction coefficient
H	= boundary-layer shape factor
$\overline{q^2}$	= twice the turbulent kinetic energy, $\overline{u'^2} + \overline{v'^2} + \overline{w'^2}$
Re_L	= Reynolds number, UL/ν
s	= average spacing between streamwise vortices
U, V, W	= mean velocity in the X, Y, Z directions, respectively
U_e	= freestream velocity in the test section
U_0	= wake velocity defect
u, v, w	= instantaneous velocity in the X, Y, Z directions, respectively, e.g., $u = U + u'$
u', v', w'	= fluctuating velocity components in the X, Y, Z directions, respectively
X, Y, Z	= Cartesian coordinates for streamwise, normal, and spanwise directions, respectively
Γ	= average streamwise vortex circulation
δ_{99}	= initial boundary layer thickness
Θ	= far-field wake momentum thickness
θ	= initial boundary-layer momentum thickness
Ω_x	= mean streamwise vorticity, $\partial W/\partial Y - \partial V/\partial Z$
$\overline{()}$	= time-averaged quantity
$()_{\max}$	= maximum value at given X station

Received March 7, 1994; revision received July 20, 1994; accepted for publication July 21, 1994.

*Research Assistant, Department of Aeronautics and Astronautics, Joint Institute for Aeronautics and Acoustics; currently at Kawachi Millibioflight Project, Research Development Corp. of Japan, 4-7-6 Komaba Meguro, Tokyo 153, Japan. Member AIAA.

†Senior Research Associate, Department of Aeronautics and Astronautics, Joint Inst. for Aeronautics and Acoustics; also Research Scientist, Fluid Mechanics Laboratory, Mail Stop 260-1. Member AIAA.

Introduction

SINCE turbulent wakes are often encountered in practical aerodynamics, the ability to control their structure and growth properties would obviously have a vital impact on the performance of many vehicles. The two-dimensional structure of wakes generated by bluff bodies, such as circular cylinders, and streamlined bodies, such as airfoils and flat plates, have been widely studied over the years.[1–4] All of the earlier studies concluded that the primary structure of the plane wake consists of strong, two-dimensional spanwise vortices of alternating sign forming the familiar von Kármán vortex street.

From the outset, it was observed that the plane wake developing from laminar boundary layers also contained an additional secondary (three-dimensional) structure which was superimposed on the spanwise vortices.[5,6] Subsequent studies showed that the secondary structure was in the form of pairs of streamwise vorticity,[7–9] similar to the ones observed in plane mixing layers,[10] although two rows of streamwise vortices were observed in wakes compared to the one row in mixing layers. The origin and evolution of these naturally occurring streamwise structures in a flat plate wake were recently investigated at relatively high Reynolds numbers ($Re_b = 28{,}000$) through detailed measurements of the mean and fluctuating velocities.[11] In the formation region, the mean streamwise vorticity appeared in a well-organized, spatially-stationary arrangement in the form of quadrupoles with each quadrupole consisting of two pairs of opposite-sign mean vorticity, with like-sign vorticity located diagonally opposite one another. The quadrupoles of mean streamwise vorticity produced large spanwise variations, in the form of pinches and crests, in the cross-stream plane contours of mean velocity and Reynolds stresses. The presence of mean streamwise vorticity also had a significant effect on the wake growth and defect-decay rates, mainly by providing additional entrainment, in addition to that provided by the spanwise vortices. Although the mean streamwise vorticity decreased with downstream distance, the spanwise variations in the velocity contours were found to persist.

With the initial boundary layers tripped, spatially stationary streamwise vortex structures were not observed, and the mean

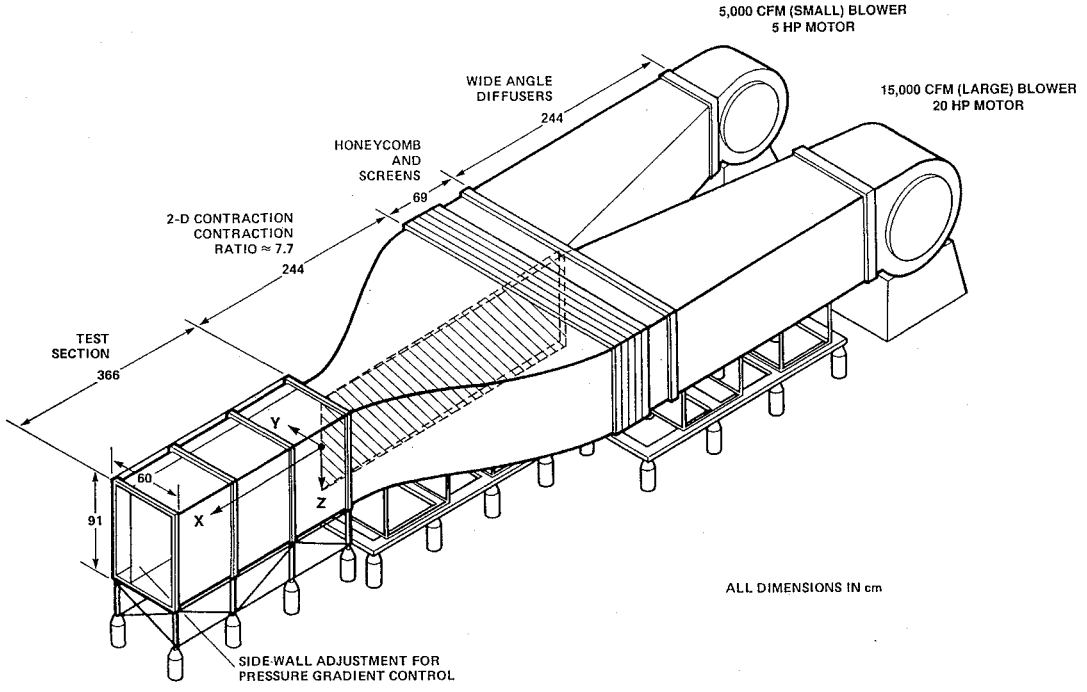

Fig. 1 Schematic of shear layer wind tunnel.

velocity and Reynolds stress contours appeared nominally two dimensional throughout the wake development.[11] Note that streamwise structures which are spatially stationary and make a continuous contribution to the secondary velocities over the full data acquisition time will always be identified in time-averaged measurements. However, relatively small-scale isolated structures, or those which meander (randomly), may not be detected in such measurements. It is, therefore, possible that time-varying streamwise vorticity is generated in the tripped wake but not captured in the time-averaged measurements. However, in a recent direct numerical simulation of a time-developing turbulent (tripped) wake, streamwise or rib vortices were not identified at all.[12,13] This is because organized spanwise structures with well-defined braid regions, where the rib vortices develop, were not formed. The wake appeared more like a "slab of turbulence with undulating boundaries."

Some attempts to lock-in the streamwise vortical structures in the initially laminar wake have also been made in flow visualization experiments. Meiburg and Lasheras[14] investigated the structure of a splitter plate wake, perturbed by a corrugated trailing edge, through inviscid vortex simulations and low Reynolds number flow visualization experiments. They found that the redistribution, reorientation, and stretching of vorticity produced counter-rotating pairs of streamwise vortices which were superimposed onto the spanwise vortices. These streamwise vortices were in the form of lambda-shaped structures and resided in the braid regions connecting adjacent (opposite-signed) spanwise vortices. Subsequent interaction of the streamwise and spanwise structures led to the formation of closed vortex loops. In terms of the streamwise development, Breidenthal[15] examined the structure in both a wake and a mixing layer formed downstream of a splitter plate with a spanwise varying trailing edge consisting of periodic tabs, and found that the wake, unlike the mixing layer, "remembered" the initial perturbation, and its distorted structure persisted into the downstream region. These results suggested that the presence of only one or both signs of spanwise vorticity may be of fundamental importance in determining the stability and spanwise structure of the vorticity field.

The main objective of the present study was to investigate the effects of streamwise vortex injection on the three-dimensional structure and development of a plane wake developing from turbulent boundary layers at relatively high Reynolds numbers ($Re_b \approx 30{,}000$). In particular, the objective was to investigate the effects of injected streamwise vorticity on the wake growth rate and turbulence structure. The behavior of the injected vorticity was also to be compared to that occurring naturally in the initially laminar case. An array of relatively strong streamwise vortices, in counter-rotating pairs, was generated by attaching a corrugated extension to a splitter plate trailing edge.

Experimental Apparatus and Techniques

The experiments were performed in a shear-layer wind tunnel (Fig. 1), consisting of two separate legs, each independently driven by a centrifugal blower.[16] The two streams merge in the test section, downstream of a sharp trailing edge of a slowly tapering splitter plate with an included angle of 1 deg. The test section is 36 cm wide in the cross-stream (Y) direction, 91 cm high in the spanwise (Z) direction, and 3.7 m long in the streamwise (X) direction. The sidewall on the small blower side is slotted, for probe access, and is flexible, for pressure gradient control. For each phase of the present experiments (with and without vorticity injection), this wall was adjusted to give a nominally zero streamwise pressure gradient.

In the present study, the two sides of the wind tunnel were run at freestream velocities (U_e) in the test section of 9 m/s. At these operating conditions, the measured streamwise turbulence intensity level (u'/U_e) was about 0.15%, and the transverse levels (v'/U_e and w'/U_e) were about 0.05%. The mean core flow in the test section was found to be uniform to within 0.5%, and the crossflow angles were less than 0.25 deg.

The boundary layers on the splitter plate were tripped using a 1.5-mm-diam round wire glued to each side of the splitter plate at a location 21 cm upstream of the trailing edge. The boundary-layer properties, measured at the splitter plate trailing edge in the absence of the corrugation, and averaged over five spanwise locations, are given in Table 1.

For the vortex injection, an extension, corrugated in the cross-stream (Y) direction (Fig. 2), was attached to the end of the splitter plate, thus giving it a three-dimensional trailing edge. This perturbation is similar to the one investigated by Meiburg and Lasheras.[14] The corrugation induced vertical and lateral velocity components in the boundary layer such that the flow migrated toward the local trough.[17] The opposite effect took place in the other boundary layer, and the secondary flow thus generated rolled up into a streamwise vortex. Hence, each full cycle of the corrugation produced a pair of opposite-signed streamwise vortices. The wavelength of the

Table 1 Tripped initial boundary-layer properties

Condition	U_e, m/s	δ_{99}, cm	θ, cm	Re_θ	H	C_f $\times 10^3$
Large side	9.0	0.95	0.099	596	1.49	5.4
Small side	9.0	0.98	0.119	700	1.32	5.1

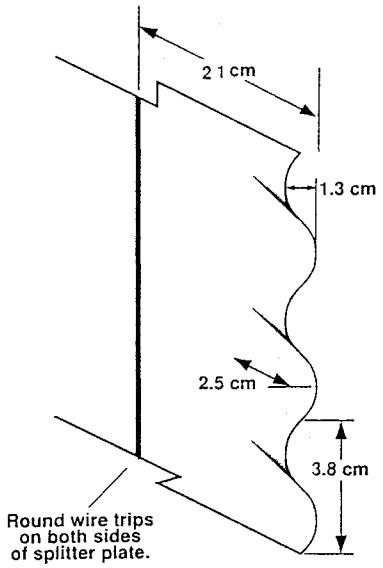

Fig. 2 Schematic of corrugation.

corrugation was chosen to approximately equal that of the natural streamwise vorticity studied previously in the initially laminar wake.[11] The amplitude of the corrugation was chosen to be of the same order as the sum of the two boundary-layer thicknesses.

Measurements were obtained using a rotatable cross-wire probe consisting of 5-μm-diam platinum-plated tungsten sensing elements approximately 1 mm in length and separated by approximately 1 mm. The signals were filtered (low-pass at 30 kHz), dc offset, and amplified by a factor of 10 before being fed into a fast sample-and-hold analog to digital (A/D) converter with 15-bit resolution and onto a Micro Vax II computer system. The probe was calibrated statically in the potential core of the flow (between the wake and wall boundary layer) assuming a cosine law response to yaw, with the effective angle determined by calibration. Note that this relatively simple calibration procedure is more than adequate for the three-dimensional flow studied here since the crossflow angles are typically less than 10 deg. The test section reference velocity (used for normalizing the data) and flow temperature (used for correcting the cross-wire data) were also acquired through the A/D system. Individual statistics were calculated by averaging over 5000 samples of cross-wire data obtained at a rate of 1500 Hz.

Data were obtained at seven streamwise stations within the test section, located between $X \approx 5$–250 cm ($X/\Theta \approx 20$–1100) downstream of the corrugated trailing edge. The measurements were made on cross-sectional (YZ) grids with the cross-wire oriented in two planes (uv and uw). This yielded all three components of mean velocity, five of the six Reynolds stresses ($\overline{v'w'}$ was not measured), and selected higher-order products. To study the streamwise development of the wake, its global properties, such as the defect and half-width, were evaluated through a spanwise averaging technique.[18] The spanwise averaged quantities were evaluated by dividing the measurements obtained on the cross-plane grid into individual Y-wise profiles. The wake properties for each profile were computed in the traditional manner and then algebraically averaged over all of the spanwise positions, giving a single value of each quantity at each streamwise location.

An error analysis, based on calibration accuracy and repeatability of measurements, indicates that mean streamwise velocity measurements with the cross wire are accurate to within 3%, whereas mean cross-stream velocities are accurate to within 10%. Reynolds normal stress measurements are accurate to within 6%, and shear stresses are accurate to within 15–20%. The measurements were corrected for mean streamwise velocity gradient ($\partial U/\partial Y$ and $\partial U/\partial Z$) effects.[11] The streamwise component of mean vorticity (Ω_x) was computed using a central difference numerical differentiation of the V and W measurements. The overall circulation (Γ) was determined from the surface integral of the streamwise vorticity field over the crossflow plane, with vorticity levels less than 20% of the maximum value being set to zero to provide immunity from noise. The integration was applied across a box on the measured grid that fully encompassed each identified vortex [that containing at least two closed vorticity contours with the spacing of the contour levels chosen to equal 10% of $(\Omega_x)_{\max}$]. The mean streamwise vorticity measurements were repeatable to within about 20% whereas the circulation measurements were repeatable to within about 25%.

Results and Discussion

All of the streamwise distances (X) in the present paper and some of the wake properties are normalized by the far-field momentum thickness (Θ) of the wake. The streamwise distributions of the momentum thicknesses were found to achieve approximately constant levels in the far-field region, giving the values $\Theta = 0.2$, 0.23, and 0.24 cm for the undisturbed untripped, undisturbed tripped, and forced cases, respectively.[11] In the present study, the streamwise domain, $X/\Theta > 500$, is defined as the *far-field* region whereas the domain, $X/\Theta < 500$ is defined as the *near-field* region.

The mean streamwise velocity contours (U/U_e) at four representative stations within the range $X/\Theta = 100$–1030 are presented in Figs. 3a–3d. A sinusoidal-type spanwise distortion is evident at the first station, with about two wavelengths captured in the measured spanwise domain. This is not too surprising since the row of opposite-signed streamwise vortices would be expected to produce an alternating "upwash/downwash-type" momentum transport. The distortion is symmetric about the wake centerline ($Y = 0$), and local maxima in the velocity defect are observed at locations where the streamwise vortices would be expected to reside. Farther downstream, the distortion becomes less severe, although its sinusoidal shape persists right up to the last measurement location ($X/\Theta = 1030$). Toward the end of the measurement domain, a higher wavelength distortion is also evident, superimposed on that produced by the injected vorticity. The mean velocity contours suggest that the spanwise wavelength of the original distortion is roughly constant with streamwise distance, implying that the spacing of the streamwise vortices is maintained. As expected, the wake defect decays with streamwise distance, from about 14% of the freestream velocity at $X/\Theta = 20$ to 5% at $X/\Theta = 1030$.

The distributions of the turbulence quantities in the wake are also affected by the injected streamwise vorticity. Since the effects on all of the Reynolds stresses were qualitatively similar,[11] only the primary shear stress ($\overline{u'v'}/U_e^2$) results are presented here. Contours of the primary shear stress at the same four streamwise locations as the mean velocity are presented in Figs. 4a–4d. At the first station, local peaks of $\overline{u'v'}$ of both signs are observed. The peaks are generally located in regions of high mean shear ($\partial U/\partial Y$) which obviously leads to higher production (through the $\overline{v'^2}\partial U/\partial Y$ term in the $\overline{u'v'}$ transport equation). The shear stress contours exhibit a sinusoidal variation downstream of $X/\Theta = 350$ with positive and negative ridges of $\overline{u'v'}$, of about equal strength, on either side of the wake centerline. As with the mean velocity contours, the distortion in the $\overline{u'v'}$ contours persists up to the end of the measurement domain, and a larger wavelength distortion becomes apparent. It is possible that this larger wavelength distortion is a result of a slight (imperceptible) bowing of the corrugation since wakes tend to be very sensitive to initial conditions. Presumably, it only becomes apparent in the far-field region since by then the stronger distortion due to the streamwise vortices has weakened considerably.

The distortions in the mean velocity and Reynolds stress contours are obviously a result of the injected streamwise vorticity. The mean streamwise vorticity contours for four streamwise locations in the region, $X/\Theta = 20$–350, are presented in Figs. 5a–5d. As expected, a single row, consisting of counter-rotating pairs of streamwise vortices of about equal strength, is generated by the corrugation. The mean streamwise vorticity contours are elongated in

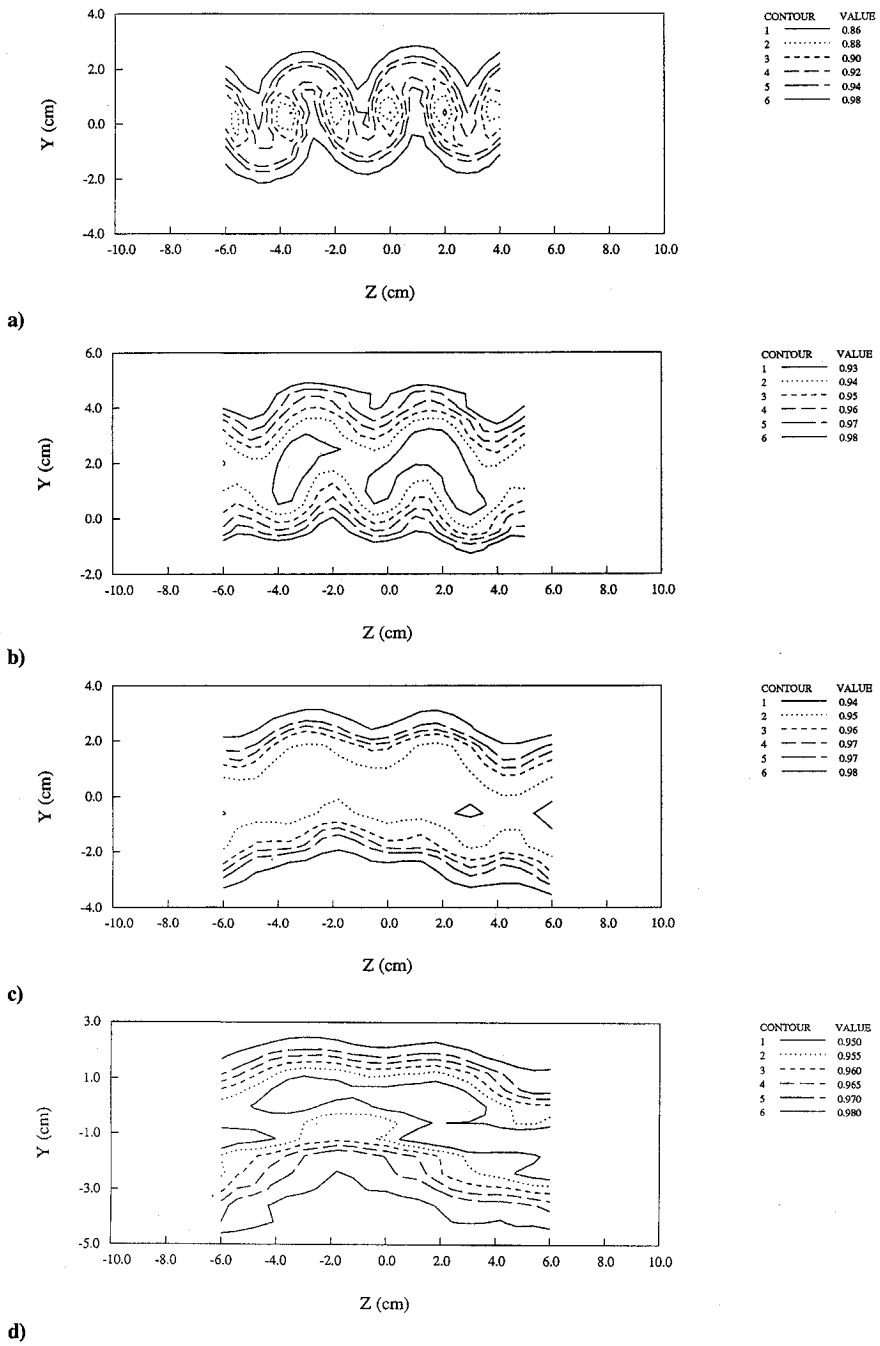

Fig. 3 Mean streamwise velocity (U/U_e) contours: a) X/Θ = 100, b) X/Θ = 350, c) X/Θ = 650, and d) X/Θ = 1030.

the vertical (Y) direction presumably due to the apparent meander that the probe sees as the streamwise vortices ride over the two rows of spanwise (von Kármán) vortices. The mean streamwise vorticity is clearly decreasing rapidly with increasing streamwise distance, although the scale of the structures and the spacing between them is maintained. Beyond $X/\Theta \approx 500$, the mean streamwise vorticity had reduced to levels comparable to the noise in the measurement scheme.

To study the evolution of the mean streamwise vorticity in a more quantitative manner, the streamwise development of the peak mean vorticity, average circulation, and vortex spacing are plotted in Figs. 6a–6c, respectively. Also shown in these figures for comparison are data for the undisturbed plane wake developing from laminar initial boundary layers[11]; recall that spatially stationary streamwise vorticity was only generated in the wake with untripped initial boundary layers and not in the tripped wake. The development of the peak mean streamwise vorticity, averaged over all vortices identified at a given station, is plotted on a log-log scale in Fig. 6a. In the region, $X/\Theta < 100$, the peak levels of the injected vorticity are slightly higher compared to those of the natural vorticity. However, the rates of reduction are different for the two cases such that the peak levels are comparable at $X/\Theta \approx 100$–300 and they become slightly lower for the injected vorticity at $X/\Theta \approx 300$–500. Thus, the overall reduction rate for the mean streamwise vorticity in the forced wake is slightly higher than that of the natural mean vorticity in the unforced wake.

The streamwise evolution of the average circulation per vortical structure is presented in Fig. 6b. The circulation for each vortical structure is evaluated as described earlier, and the absolute values are then averaged over all structures at a given streamwise location. The average circulation for the undisturbed case is approximately constant, as would be expected. The circulation for the injected vortices is much higher initially (by a factor of about 10), but then drops rapidly such that by $X/\Theta \approx 400$, the levels for the two cases are comparable. It seems as though the corrugation produces relatively diffuse but strong vortices which the wake cannot support, and so they weaken rapidly, at least until their strength becomes comparable to that of the natural structures.

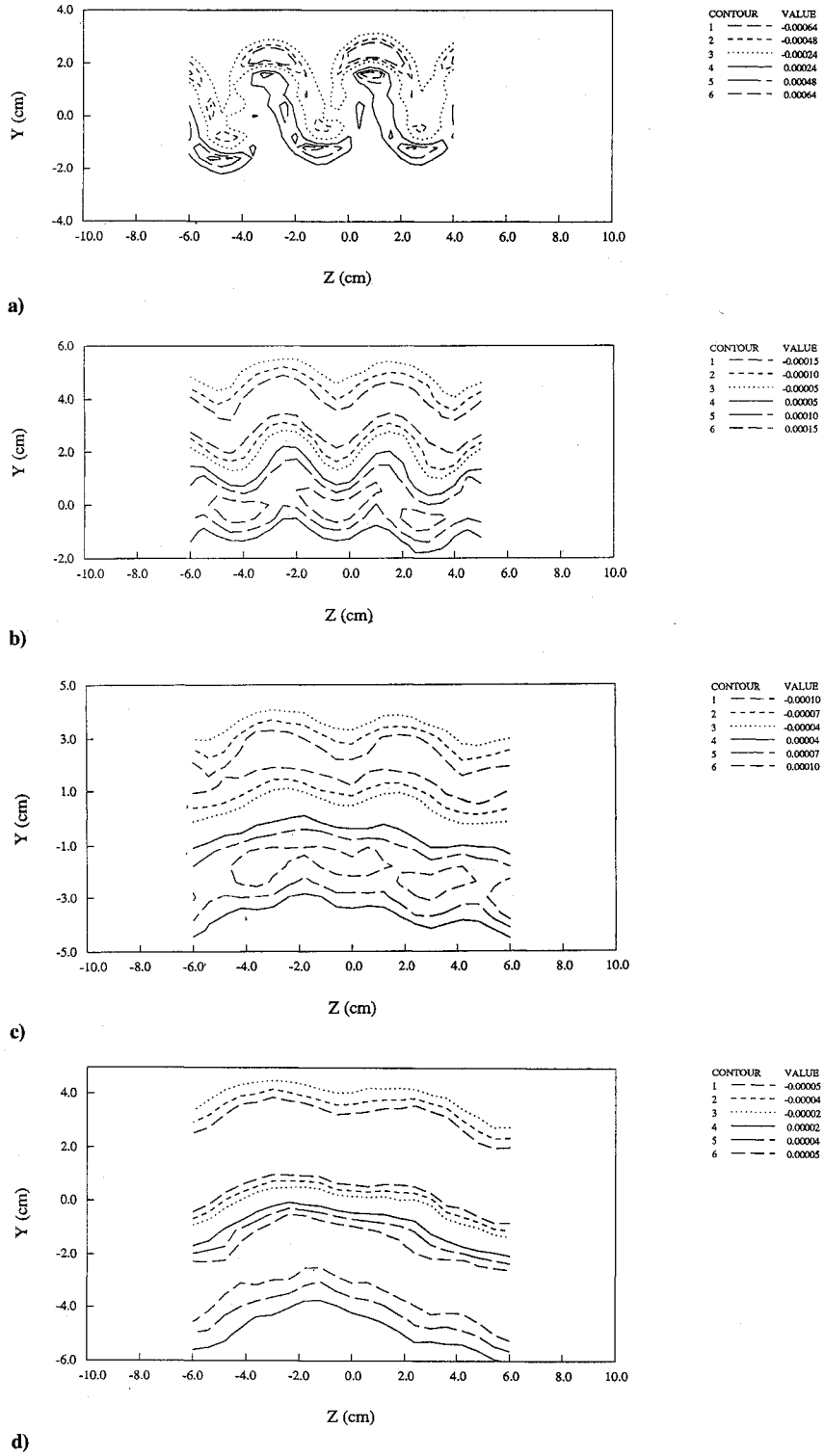

Fig. 4 Primary shear stress ($\overline{u'v'}/U_e^2$) contours: a) X/Θ = 100, b) X/Θ = 350, c) X/Θ = 650, and d) X/Θ = 1030.

The development of the mean spacing of the streamwise vortical structures, calculated by dividing the measured span by the number of identified structures, is shown in Fig. 6c. The spacing for the structures in the undisturbed case clearly increases in a stepwise fashion. However, that for the injected vorticity remains constant throughout the measured domain. This may simply be due to the fact that the injected vortices are of equal strength and spacing, unlike the naturally occurring structures,[11] and remain that way so there is no tendency for self-induced motion. An irregular spanwise distribution and induced motion are necessary for the identified mechanisms (vortex amalgamation and annihilation) which can lead to a change in the scale and, hence, spacing of the streamwise vortical structures.[11]

The streamwise evolution of some of the wake global properties are presented in Figs. 7 and 8. All of the quantities are spanwise averaged, as already described, and the results for the wake with streamwise vorticity injection are compared to those for the same wake (tripped initial boundary layers) without the vorticity injection. The streamwise development of the wake half-width for the two cases is shown in Fig. 7a. The half-width is defined as the distance between the Y locations at which the mean velocity is equal to $(U_e - U_0/2)$. The development of the half-width for the undisturbed case was found to agree well with the half-power-law relation for a self-similar wake.[11] The wake with vorticity injection grows very rapidly in the region $X/\Theta < 300$. This result was not too

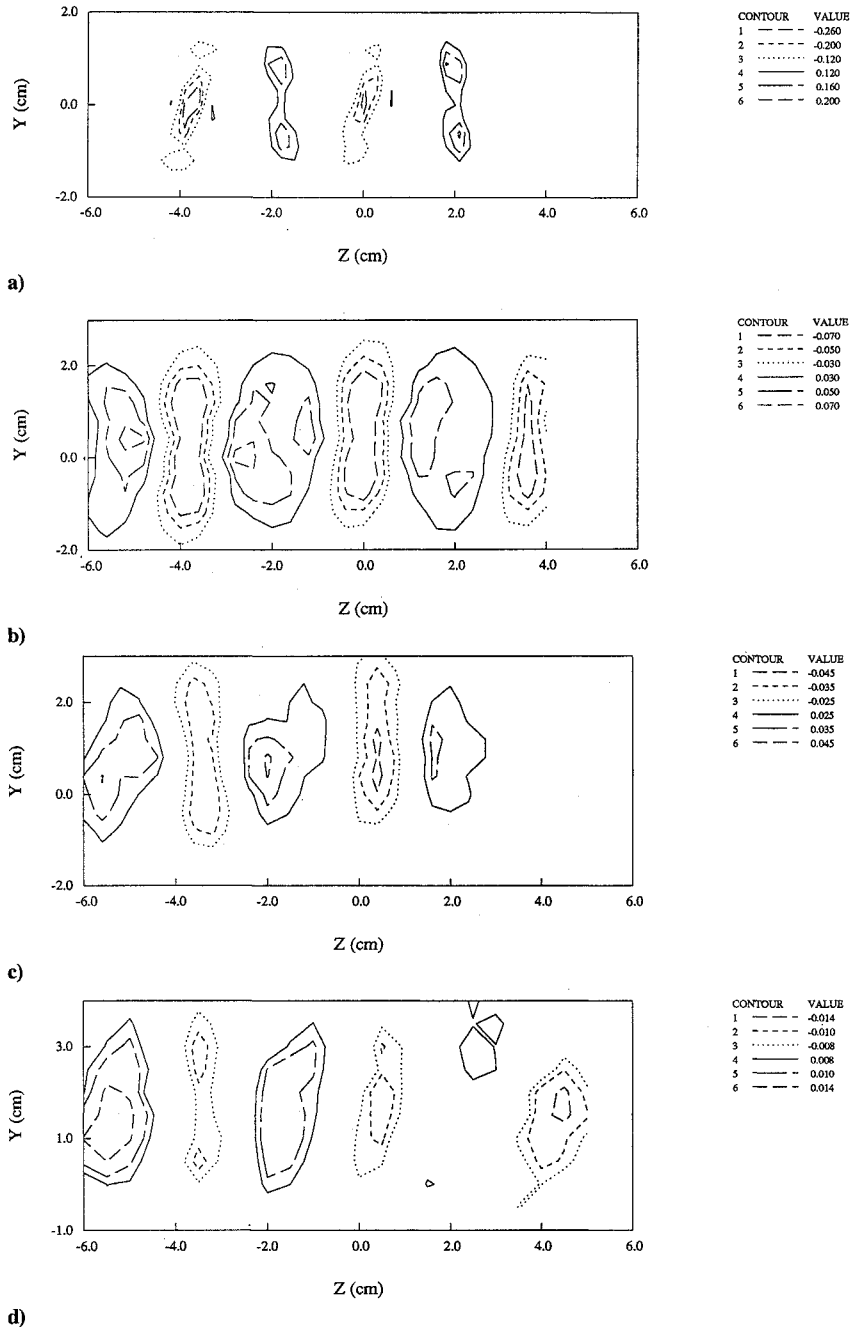

Fig. 5 Mean streamwise vorticity (Ω_x/U_e, cm^{-1}) contours: a) X/Θ = 20, b) X/Θ = 100, c) X/Θ = 180, and d) X/Θ = 350.

surprising since the injected streamwise vorticity is expected to entrain additional fluid (in addition to that by the spanwise vortices), thus leading to a higher growth rate and thickness. In the region $300 < X/\Theta < 600$, the growth rates for the two wakes are comparable. However, farther downstream, the forced wake growth rate is *reduced* drastically compared to that of the undisturbed wake and, consequently, the half-widths are comparable by the end of the measurement domain ($X/\Theta \approx 1000$). The reduction in forced wake growth rate occurs in the region where the mean streamwise vorticity has also decreased to negligible levels. This result lends further support to the argument that the higher forced wake growth rate in the initial region is due to additional entrainment by the injected streamwise vorticity.

The streamwise development of the wake velocity defect (U_0) for the two cases is presented in Fig. 7b. Once again, the development of the defect for the undisturbed wake agreed well with the half-power-law for a self-similar wake.[11] The main difference between the two cases is in the rate at which the defect falls off. The defect in the forced case decreases rapidly in the region $X/\Theta < 300$, again mainly due to the effects of the injected streamwise vorticity in entraining more fluid, thus filling in the defect faster. Beyond $X/\Theta \approx 400$, the rate of defect decay in the forced wake is slightly lower than that of the undisturbed case, thus making the defect levels for the two cases comparable in the far-field region.

Since the streamwise evolution of the forced wake half-width and velocity defect are affected significantly, it seems conceivable that the Reynolds stress levels must also exhibit some differences. This is indeed the case as shown in the streamwise development results for the maximum turbulent kinetic energy $(\overline{q^2}/U_0^2)_{\max}$ (Fig. 8a), and the maximum primary shear stress $(\overline{u'v'}/U_0^2)_{\max}$ (Fig. 8b). The Reynolds stresses are normalized by a spanwise-averaged velocity defect. The undisturbed wake levels exhibit the familiar slow rise to constant levels in the far-field region, thus showing a self-similar behavior. On the other hand, the forced wake levels clearly tend to overshoot in the near-field region and then asymptote to lower levels in the far-field region. The overshoot in the near-field region is attributed to additional production due to the mean velocity gradients (of all three mean velocities) generated in the distorted wake. The

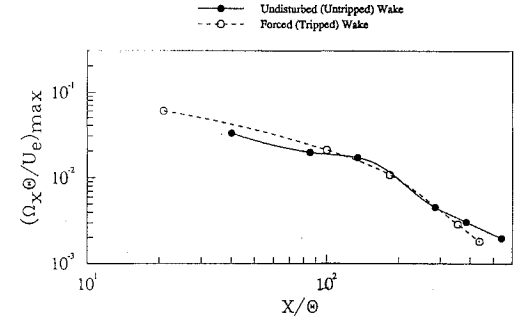

a)

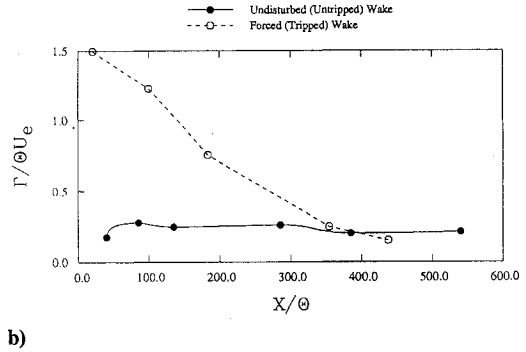

b)

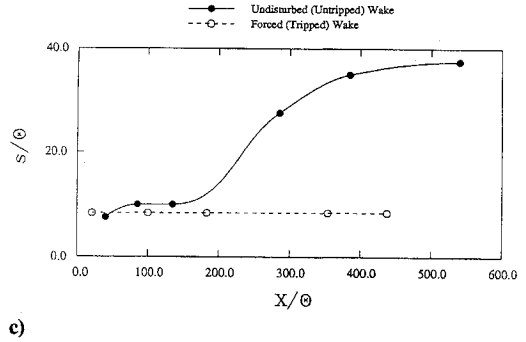

c)

Fig. 6 Streamwise development of mean streamwise vorticity properties: a) peak streamwise vorticity $[(\Omega_x\Theta/U_e)_{max}]$, b) average streamwise vortex circulation $(\Gamma/\Theta U_e)$, and c) streamwise vortex spacing (s/Θ).

lower stress levels in the far-field region are consistent with the lower growth rate. It is interesting to note that the peak Reynolds stress levels for the forced wake show no signs of recovering to the undisturbed levels, even toward the very end of the measurement domain ($X/\Theta \approx 1100$). This result reiterates the very slow recovery of a plane wake from initial perturbations.

One of the most important and interesting results from the present study is the effect of the injected streamwise vorticity on the wake growth and defect decay in the far-field region. Most of the growth of a wake occurs due to entrainment, in the form of engulfment of fluid, by the nominally two-dimensional spanwise vortical structures. In the wake developing from laminar boundary layers, the streamwise vortical structures are found to be superimposed on the spanwise (von Kármán) rollers.[14] On the other hand, streamwise vortical structures have not been observed in an undisturbed wake developing from turbulent boundary layers.[11–13] It was found in our earlier experimental studies[11] that the near-field growth and defect decay rates were significantly higher in the initially laminar wake compared to those in the turbulent case. The difference was attributed to the ability of the streamwise vortices in the initially laminar case to entrain additional fluid, thus leading to a higher growth rate and faster defect decay. Since the mean streamwise vorticity decreased with downstream distance, the growth and defect decay rates in the far-field region were found to be comparable for the tripped and untripped wakes.[11] Thus, it was expected that in the present study the injection of streamwise vorticity would also

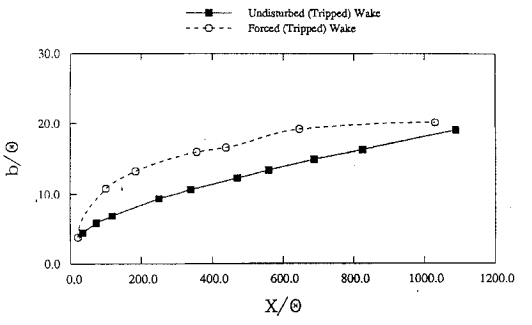

a)

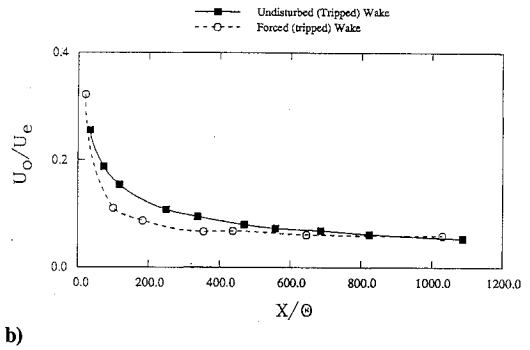

b)

Fig. 7 Streamwise development of wake global properties: a) wake half-width (b/Θ) and b) velocity defect (U_0/U_e).

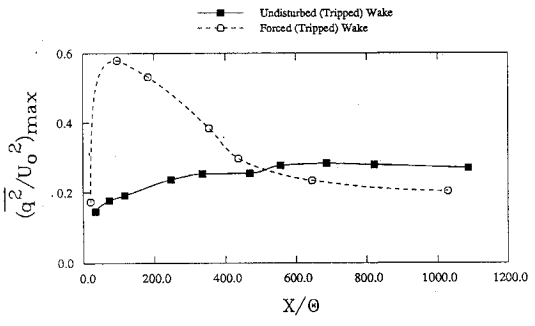

a)

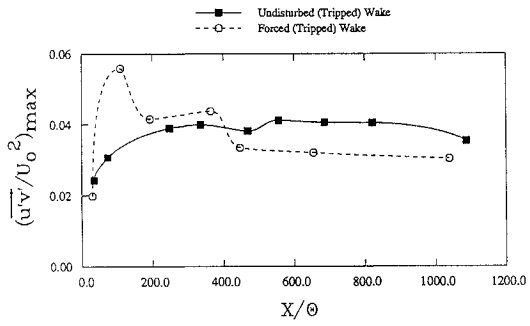

b)

Fig. 8 Streamwise development of maximum Reynolds stresses: a) maximum turbulent kinetic energy $[(q^2/U_0^2)_{max}]$ and b) maximum primary shear stress $[(\overline{u'v'}/U_0^2)_{max}]$.

increase the wake growth and defect decay rates. These effects are certainly apparent in the initial region of the forced wake (Figs. 7a and 7b). However, farther downstream, the growth and defect decay rates of the forced wake and its peak Reynolds stresses are reduced below those for the undisturbed tripped wake, a somewhat surprising result.

In the present forced wake, the relatively strong injected streamwise vorticity must be expected to affect the coherence of the span-

wise structures, based on the gross distortions in the mean velocity and Reynolds stress contours (Figs. 3 and 4). It is conceivable that less fluid would be engulfed if the coherence of the spanwise structures were reduced, thus making them more three dimensional. It is proposed here that the injected streamwise vorticity reduces entrainment by the spanwise rollers by modifying their spanwise coherence. In the near-field region, additional entrainment by the secondary structure more than makes up for this deficit. However, entrainment due to the injected streamwise vortices decreases, since they weaken rapidly with streamwise distance, but the spanwise structure recovery is slow, as partly evidenced in the contour plots of mean velocity and Reynolds stresses. As a result, the overall entrainment rate is reduced in the far-field region and, hence, the growth and defect decay rates of the wake drop.

In many ways, the effects of streamwise vorticity injection on the wake structure and development are very similar to those previously observed in mixing layers using the same spanwise perturbation mechanism.[19] The growth rate and peak Reynolds stresses in the mixing layer were also increased by vorticity injection in the near-field region and reduced in the far-field region. The injected vorticity weakens relatively quickly in both shear flows. The main difference between the effect in the wake and the mixing layer is that the mean velocity and Reynolds stress contours in the mixing layer recover to a nominally two-dimensional behavior in the far-field region, whereas those in the wake still sustain the distortions. We believe that it is the effect of the injected vorticity on the coherence of the spanwise structures that is responsible for the observed effects in both free-shear flows.

Conclusions

The effects of injecting a relatively strong array of streamwise vortices on the structure and development of a splitter plate wake originating from turbulent boundary layers have been investigated. Counter-rotating pairs of streamwise vortices were generated by a corrugation attached to the splitter plate trailing edge.

The injected vorticity produced large spanwise variations in the mean velocity and Reynolds stress contours which persisted into the far-field region ($X/\Theta > 500$). This is despite the fact that the mean streamwise vorticity decreased rapidly with streamwise distance such that it was not measurable in the far-field region. The peak mean streamwise vorticity of the injected vortices decreased somewhat faster than that of the natural vortices previously measured in undisturbed wakes developing from laminar boundary layers.[11] However, unlike the natural vorticity, the spanwise spacing of the injected vortices did not increase with streamwise distance. The main reason for the lack of change in spacing is that the uniform array of injected streamwise vortices remains more or less uniform, and there is less tendency for self-induced motions of the vortices, a necessary condition for a spanwise scale change.

The present results clearly show that the structure and growth of a turbulent wake can be effectively controlled by imposing a relatively strong streamwise vortical structure at the origin. It was expected that vorticity injection would increase wake growth and defect decay due to extra entrainment by the streamwise structures, and this was indeed observed in the near-field region ($X/\Theta < 500$). However, the far-field growth rate of the forced wake and the peak Reynolds stresses were drastically reduced over those in the undisturbed case. The rate of defect decay was also reduced somewhat in the far-field region. It is conjectured here that the injection of relatively strong streamwise vorticity at the origin leads to reduced growth and defect decay in the far-field by breaking-up the spanwise structures, making them more three dimensional and, hence, reducing their entrainment efficiency. In the near field, this effect is compensated for by increased entrainment from the streamwise structures, but this contribution is lost in the far field, where the streamwise vortical structures have weakened considerably.

Acknowledgments

This research was conducted in and supported by the Fluid Mechanics Laboratory, NASA Ames Research Center under Grant NCC-2-55. We are grateful to Richard L. LeBoeuf for reviewing an earlier draft of this paper.

References

[1]Roshko, A., "On the Development of Turbulent Wakes from Vortex Streets," NACA Rept. 1191, 1954.

[2]Taneda, S., "Downstream Development of the Wakes behind Cylinders," *Journal of Physical Society Japan*, Vol. 14, 1959, pp. 843–848.

[3]Morkovin, M., "Flow Around Circular Cylinders—a Kaleidoscope of Challenging Fluid Phenomena," *ASME Symposium on Fully Separated Flows*, American Society of Mechanical Engineers, 1964, pp. 102–118.

[4]Townsend, A. A., *Structure of Turbulent Shear Flow*, 1st ed., Cambridge Univ. Press, Cambridge, England, UK, 1956.

[5]Grant, H. L., "The Large Eddies of Turbulent Motion," *Journal of Fluid Mechanics*, Vol. 4, 1958, pp. 149–190.

[6]Gerrard, J. H., "The Three-Dimensional Structure of the Wake of a Circular Cylinder," *Journal of Fluid Mechanics*, Vol. 25, 1966, pp. 143–164.

[7]Wei, T., and Smith, C. R., "Secondary Vortices in the Wake of Circular Cylinders," *Journal of Fluid Mechanics*, Vol. 169, 1986, pp. 513–533.

[8]Hayakawa, M., and Hussain, F., "Three-Dimensionality of Organized Structures in a Plane Turbulent Wake," *Journal of Fluid Mechanics*, Vol. 206, 1989, pp. 375–404.

[9]Williamson, C. H. K., "The Natural and Forced Formation of Spot-Like 'Vortex Dislocations' in the Transition of a Wake," *Journal of Fluid Mechanics*, Vol. 243, 1992, pp. 393–441.

[10]Bell, J. H., and Mehta, R. D., "Measurements of the Streamwise Vortical Structures in a Plane Mixing Layer," *Journal of Fluid Mechanics*, Vol. 239, 1992, pp. 213–248.

[11]Weygandt, J. H., and Mehta, R. D., "Three-dimensional Structure of Straight and Curved Plane Wakes," Dept. of Aeronautics and Astronautics, JIAA TR-110, Stanford Univ., Stanford, CA, Sept. 1993; also *Journal of Fluid Mechanics*, Vol. 282, 1995, pp. 279–311.

[12]Rogers, M. M., and Moser, R. D., "The Evolution of a Self-Similar Turbulent Plane Wake," *Bulletin of the American Physical Society*, Vol. 38, 1993, p. 2271.

[13]Moser, R. D., and Rogers, M. M., "Direct Simulation of a Self-Similar Plane Wake," AGARD Symposium on Application of Direct and Large Eddy Simulation, Crete, Greece, April, 1994.

[14]Meiburg, E., and Lasheras, J. C., "Experimental and Numerical Investigation of the Three-Dimensional Transition in Plane Wakes," *Journal of Fluid Mechanics*, Vol. 190, 1988, pp. 1–37.

[15]Breidenthal, R., "Response of Plane Shear Layers and Wakes to Strong Three-Dimensional Disturbances," *Physics of Fluids A*, Vol. 23, 1980, pp. 1929–1934.

[16]Bell, J. H., and Mehta, R. D., "Design and Calibration of the Mixing Layer Wind Tunnel," *Dept. of Aeronautics and Astronautics*, JIAA TR-89, Stanford Univ., Stanford, CA, May 1989.

[17]Eckerle, W. A., Sheibani, H., and Awad, J., "Experimental Measurement of the Vortex Development Downstream of a Lobed Mixer," *Transactions ASME: Journal of Engineering for Gas Turbines and Power*, Vol. 114, 1992, pp. 63–71.

[18]Bell, J. H., Plesniak, M. W., and Mehta, R. D., "Spanwise Averaging of Plane Mixing Layer Properties," *AIAA Journal*, Vol. 30, 1992, pp. 835–837.

[19]Bell, J. H., and Mehta, R. D., "Effects of Imposed Spanwise Perturbations on Plane Mixing Layer Structure," *Journal of Fluid Mechanics*, Vol. 257, 1993, pp. 33–63.